Supporting information

Highly stable single Pt atomic sites anchored on aniline-stacked graphene for the hydrogen evolution reaction

Shenghua Ye, Feiyan Luo, Qianling Zhang, Pingyu Zhang, Tingting Xu, Qi Wang, Dongsheng He, Licheng Guo, Yu Zhang, Chuanxin He, Xiaoping Ouyang, Meng Gu,* Jianhong Liu* and Xueliang Sun*

Contents

Table

Table S1. EXAFS fitting parameters for the Pt L_3-edges of the Pt SASs/AG and Pt/C.

Sample	path	N	R (Å)	$\Sigma/10^{-3}$Å^2	ΔE_0 (eV)	R factor/10^{-3}
Pt SASs/AG	Pt–N	4.3	2.03	7.4	14.7	4.0
Pt/C	Pt–Pt	12.0	2.76	5.0	8.5	2.4

Table S2. EXAFS fitting parameters for the Pt L_3-edges of the Pt SASs/AG before and after durability testing.

Sample	path	N	R (Å)	$\Sigma/10^{-3}$Å^2	ΔE_0 (eV)	R factor/10^{-3}
As-prepared Pt SASs/AG	Pt–N	4.3	2.03	7.4	14.7	4.0
Pt SASs/AG after durability test	Pt–N	4.5	2.03	7.4	14.7	4.0

Figures

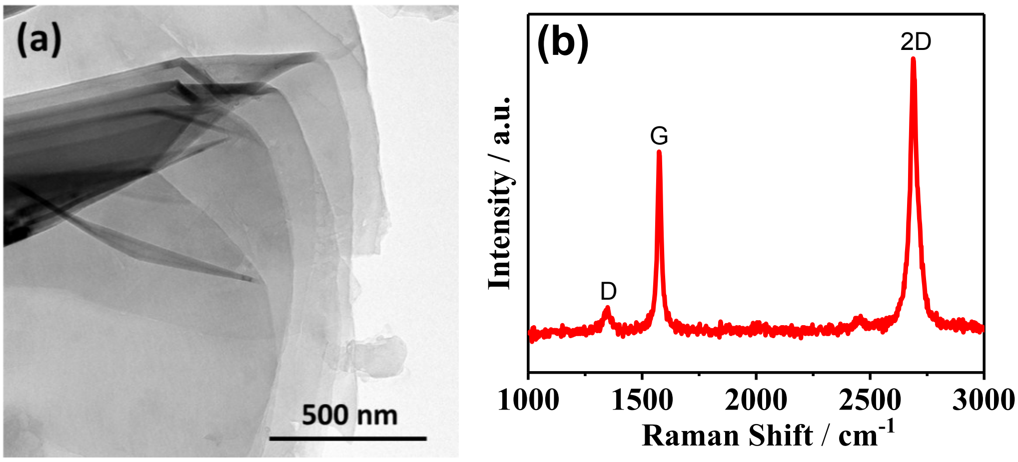

Fig. S1 (a) TEM image, and (b) Raman spectrum of graphene.

The low I_D/I_G and intensive 2D peaks with narrow FWHM indicate that low defect and high quality of graphene.

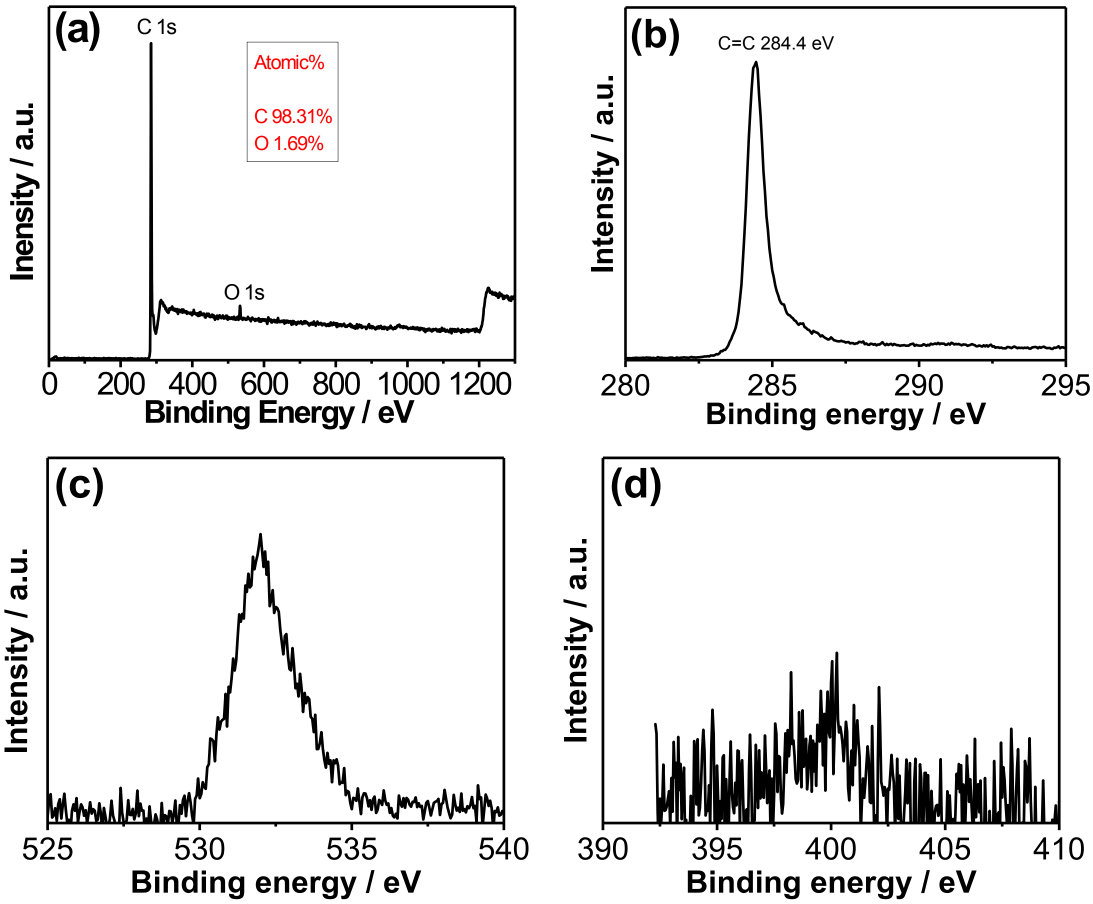

Fig. S2 XPS spectra of (a) survey, (b) C1s, (c) O1s, and (d) N 1s of graphene

The oxygen in graphene is as low as 1.69 at%, and the binding energy of O 1s is located at ~532 eV, which suggests that the oxygen is originated from absorbed H_2O on the surface. Moreover, the content of nitrogen is negligible from the spectra of survey and N 1s, indicates that the graphene is pure without doping of heteroatom.

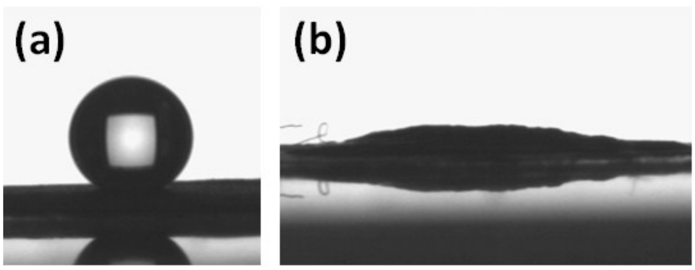

Fig. S3 Water-contact angle of (a) graphene and (b) aniline-stacked graphene.

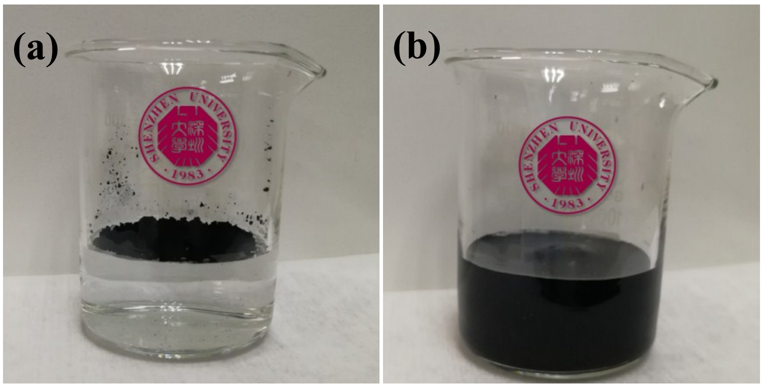

Fig. S4 Photos of (a) graphene–water suspension and (b) aniline-stacked graphene dispersion.

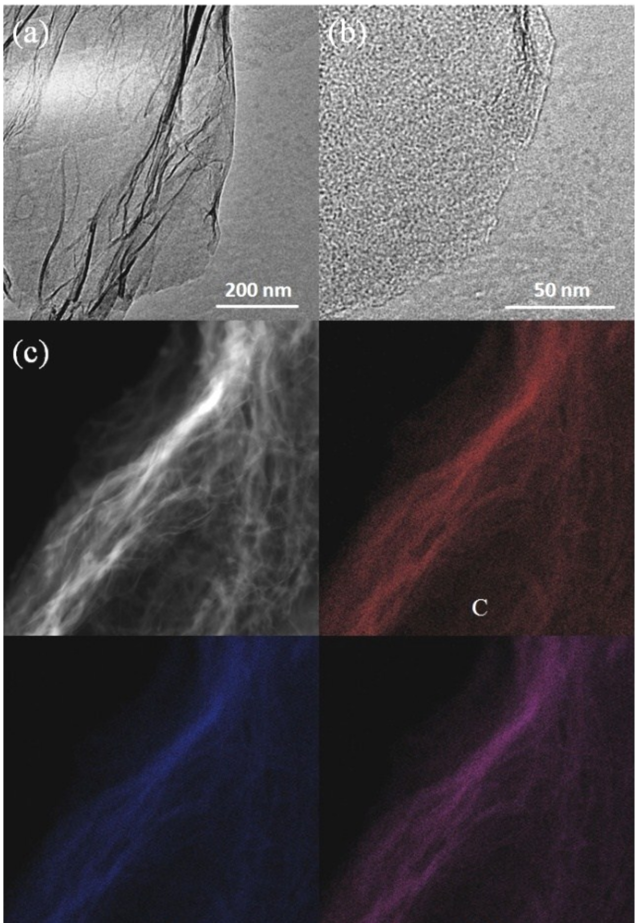

Fig. S5 (a) TEM, (b) HRTEM images, and (c) elemental mapping images of C and N of AG.

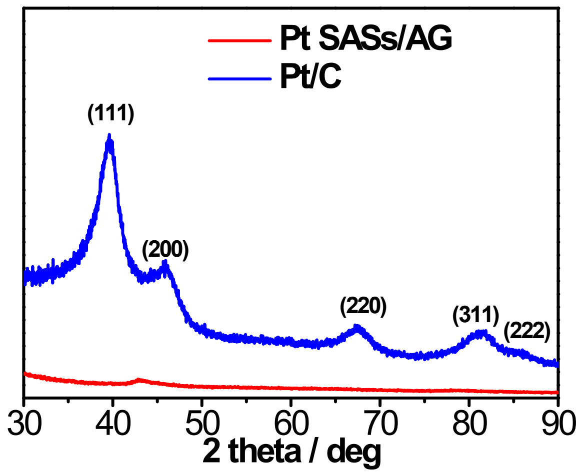

Fig. S6 XRD patterns of Pt SASs/AG and Pt/C (PDF#65-2868).

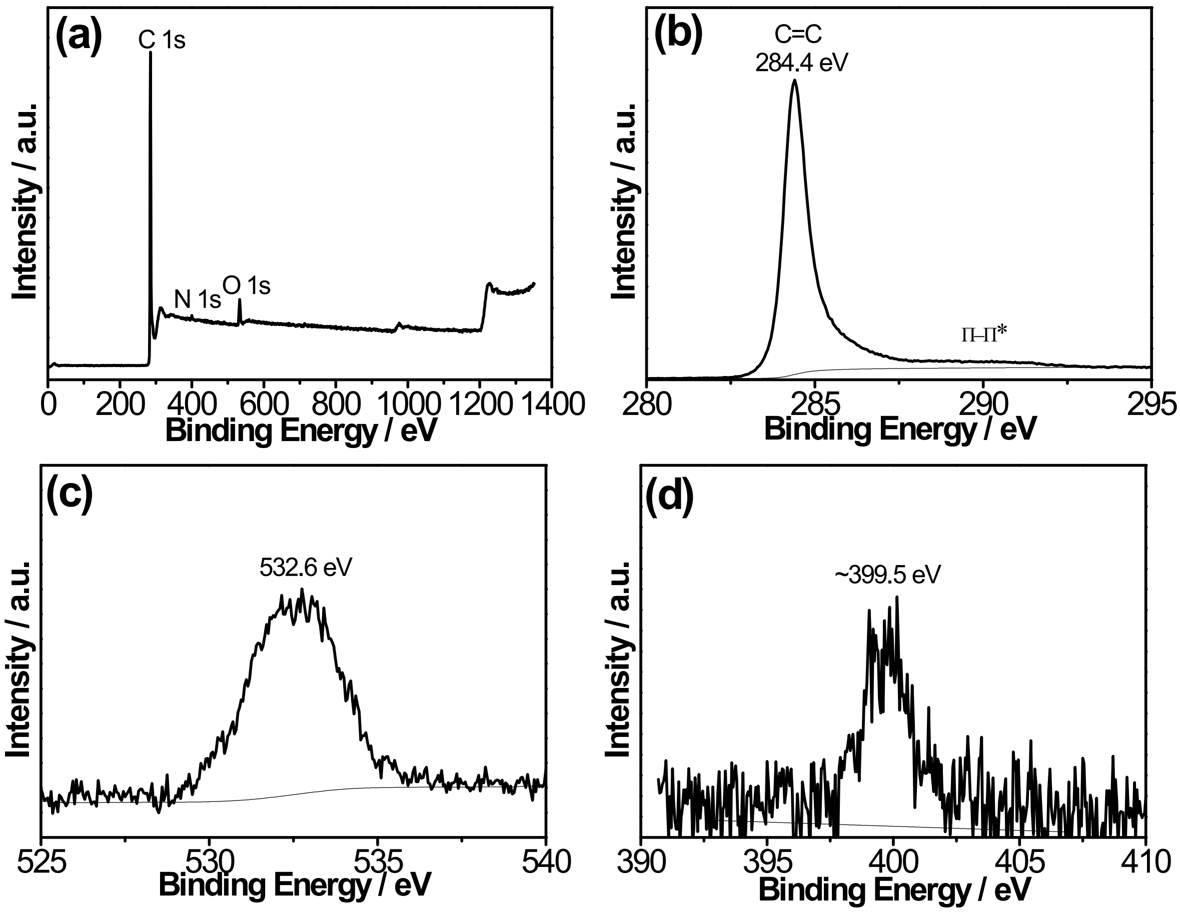

Fig. S7 XPS spectra of (a) survey, (b) C1s, (c) O1s, and (d) N 1s of AG.

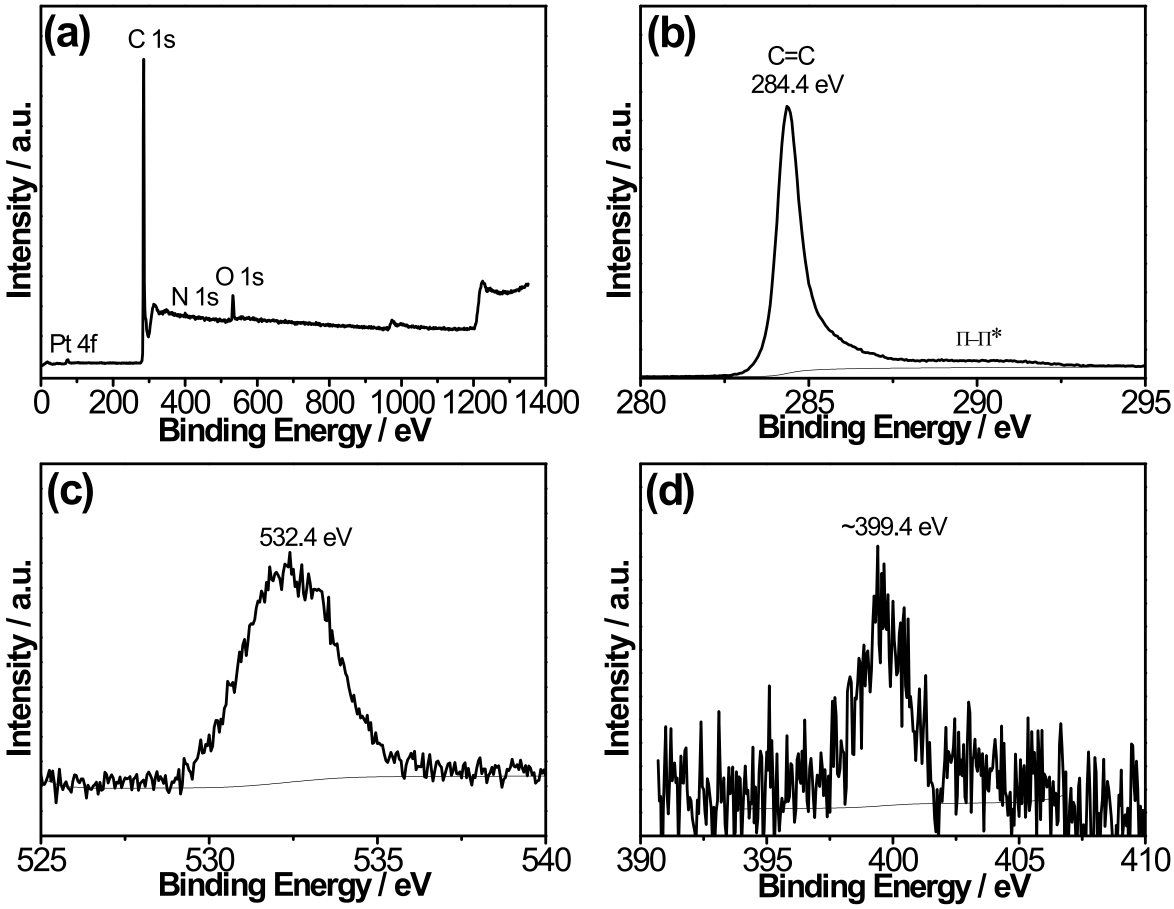

Fig. S8 XPS spectra of (a) survey, (b) C1s, (c) O1s and (d) N 1s of Pt SASs/AG.

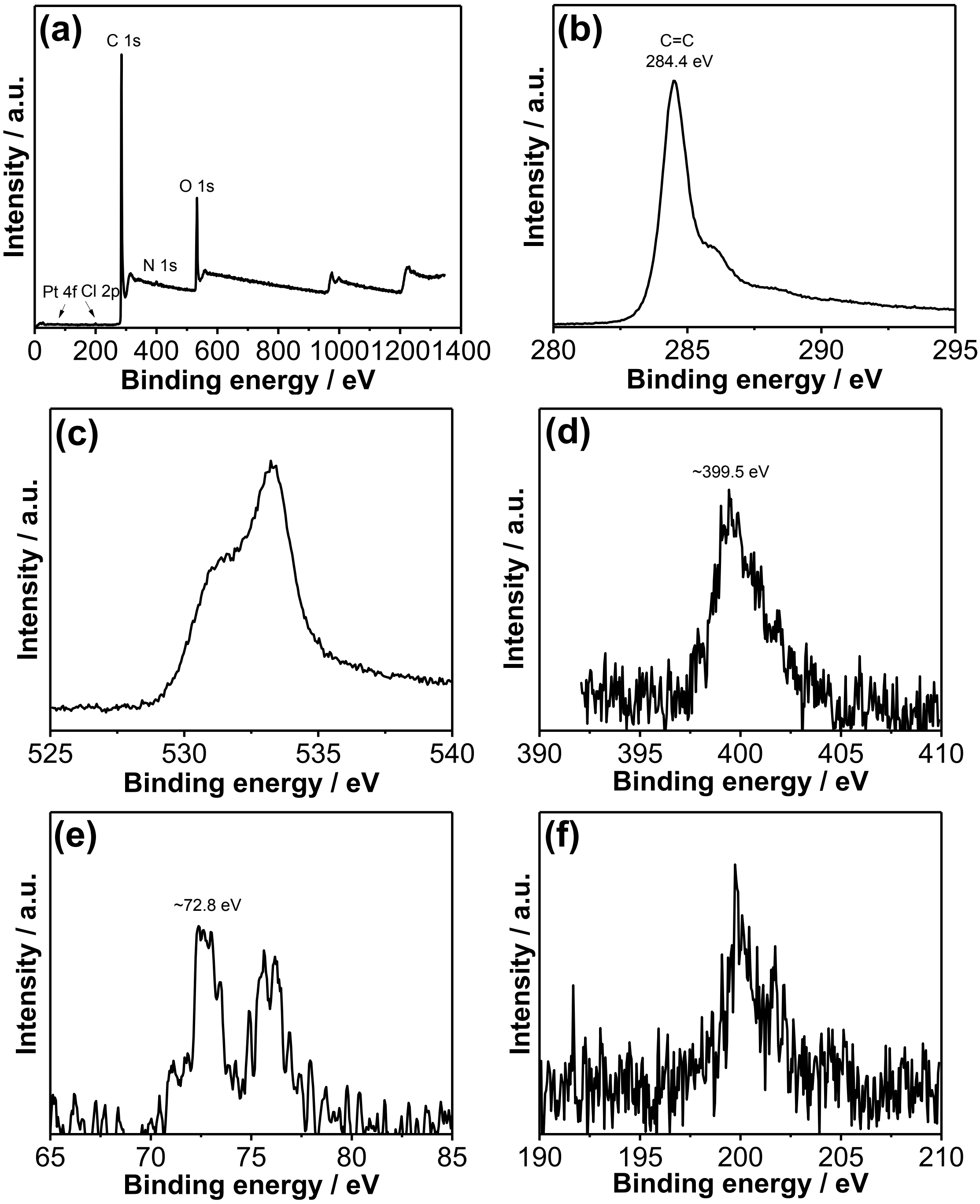

Fig. S9 XPS spectra of (a) survey, (b) C1s, (c) O1s, (d) N 1s, (e) Pt 4f and (f) Cl 2p of Pt SASs/AG before microwave irradiation.

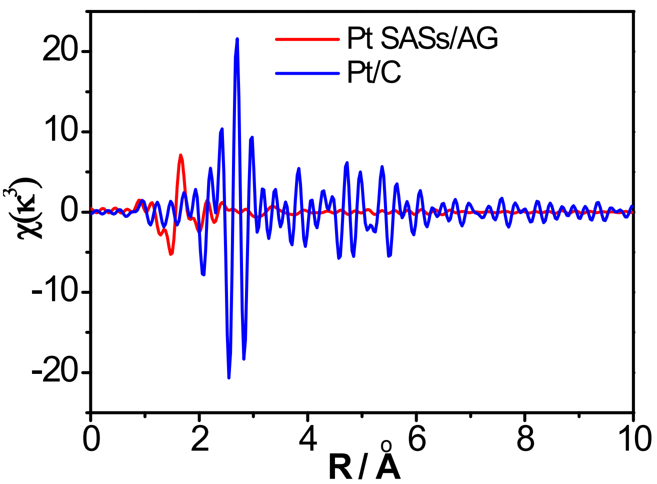

Fig. S10 Extended XAFS spectra of Pt SASs/AG and Pt/C.

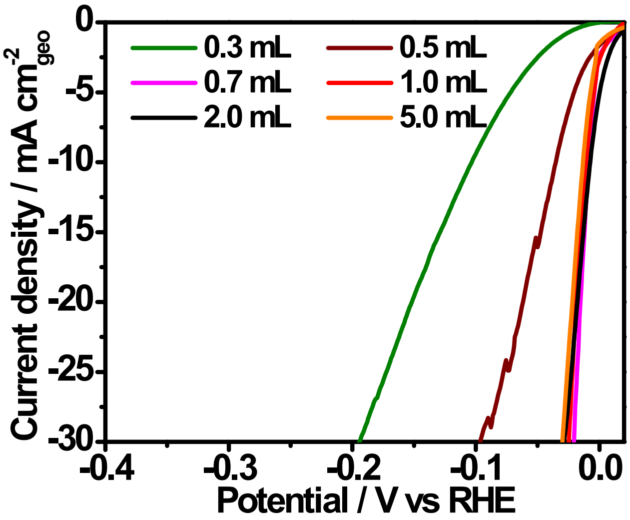

Fig. S11 LSV curves of Pt SASs/AG prepared by different volumes of H_2PtCl_6 solution with iR corrction.

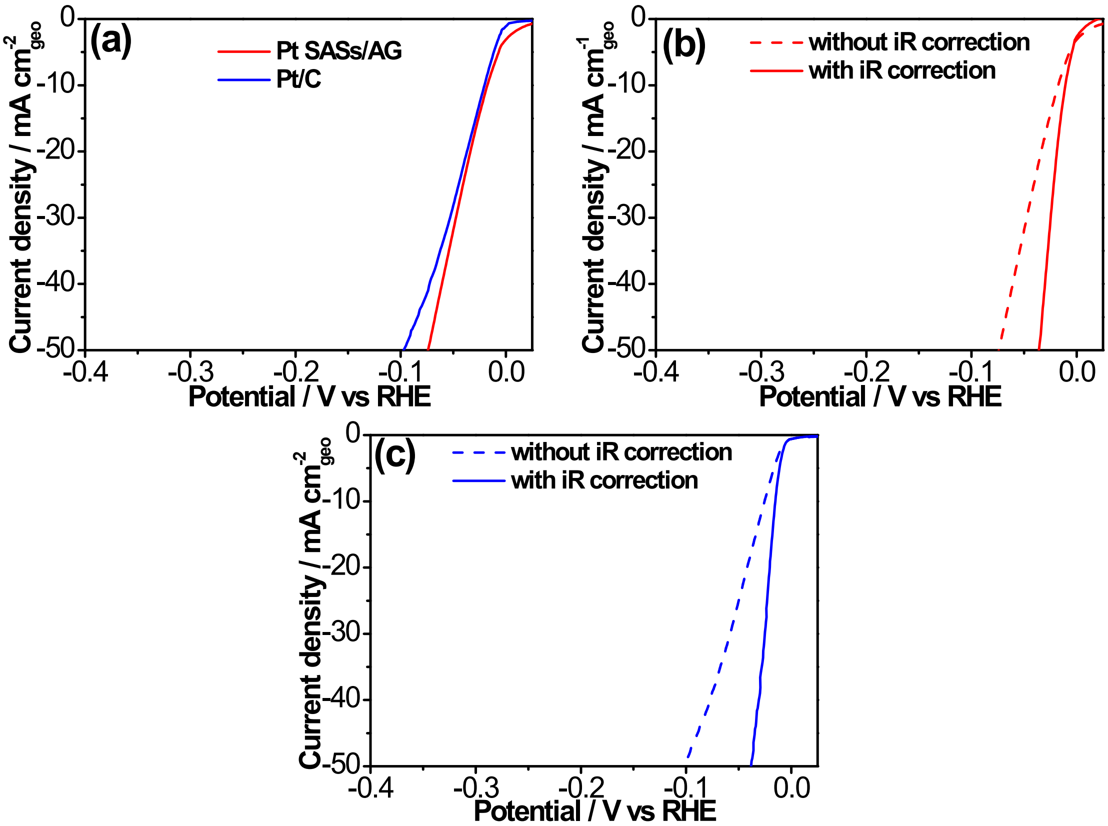

Fig. S12 (a) LSV curves of Pt SASs/AG and Pt/C before the iR correction; LSV curves of (b) Pt SASs/AG, and (c) Pt/C before and after the iR correction.

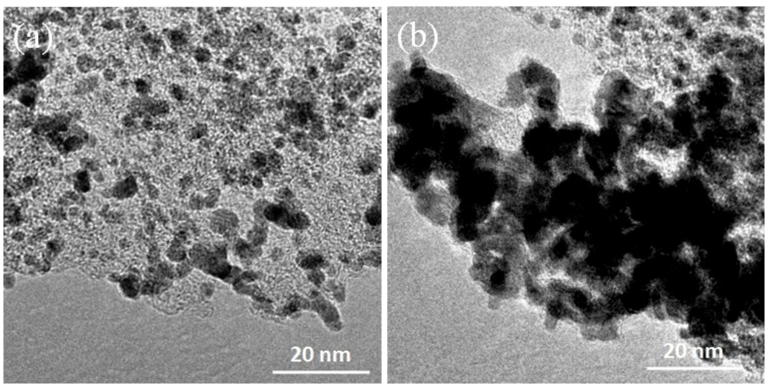

Fig. S13 TEM images of Pt/C (a) before and (b) after durability testing.

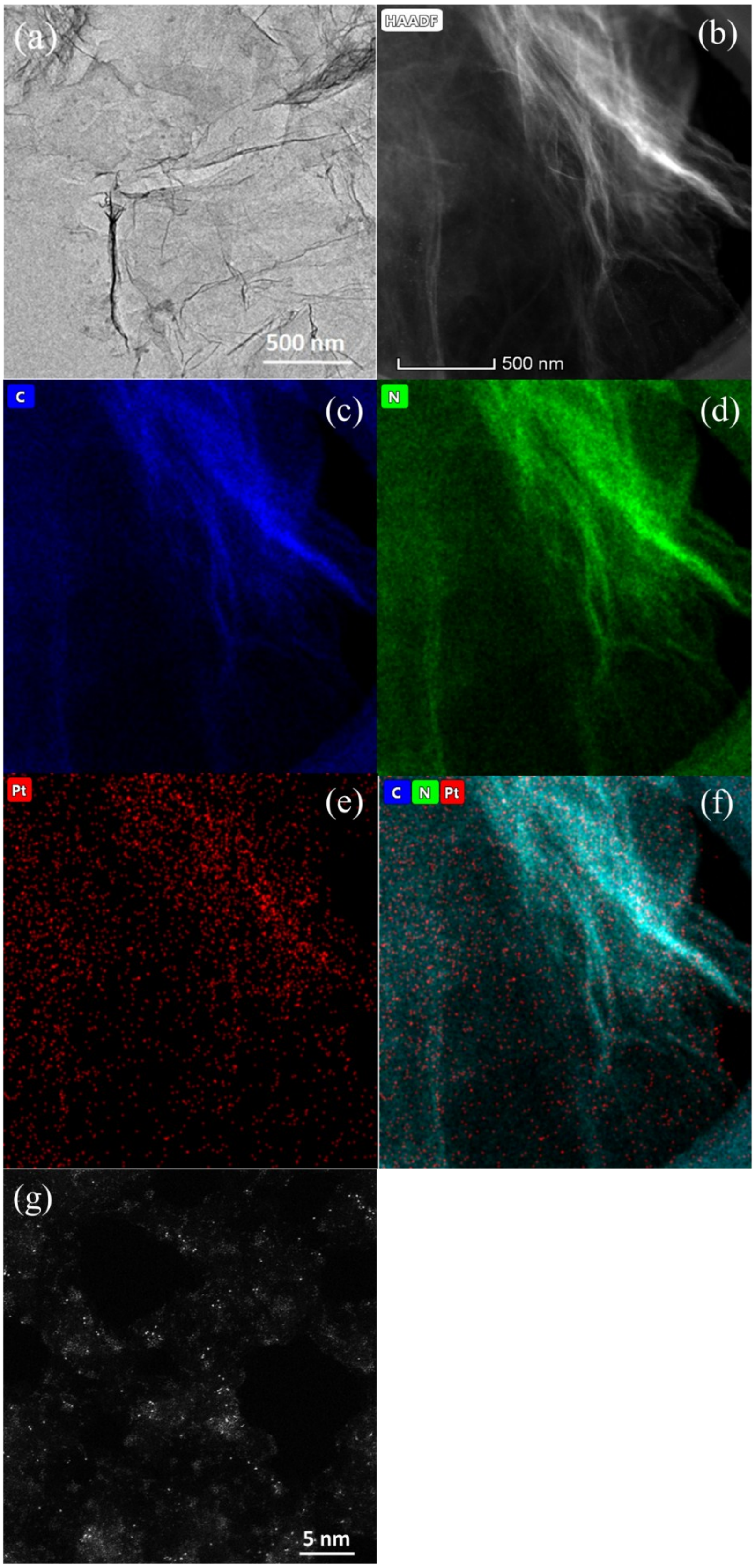

Fig. S14 (a) TEM image, (b) HAADA-STEM images and corresponding elemental mapping of (c-f) C, N, Pt and (g) AC HAADA-STEM images of Pt SASs/AG after durability testing.

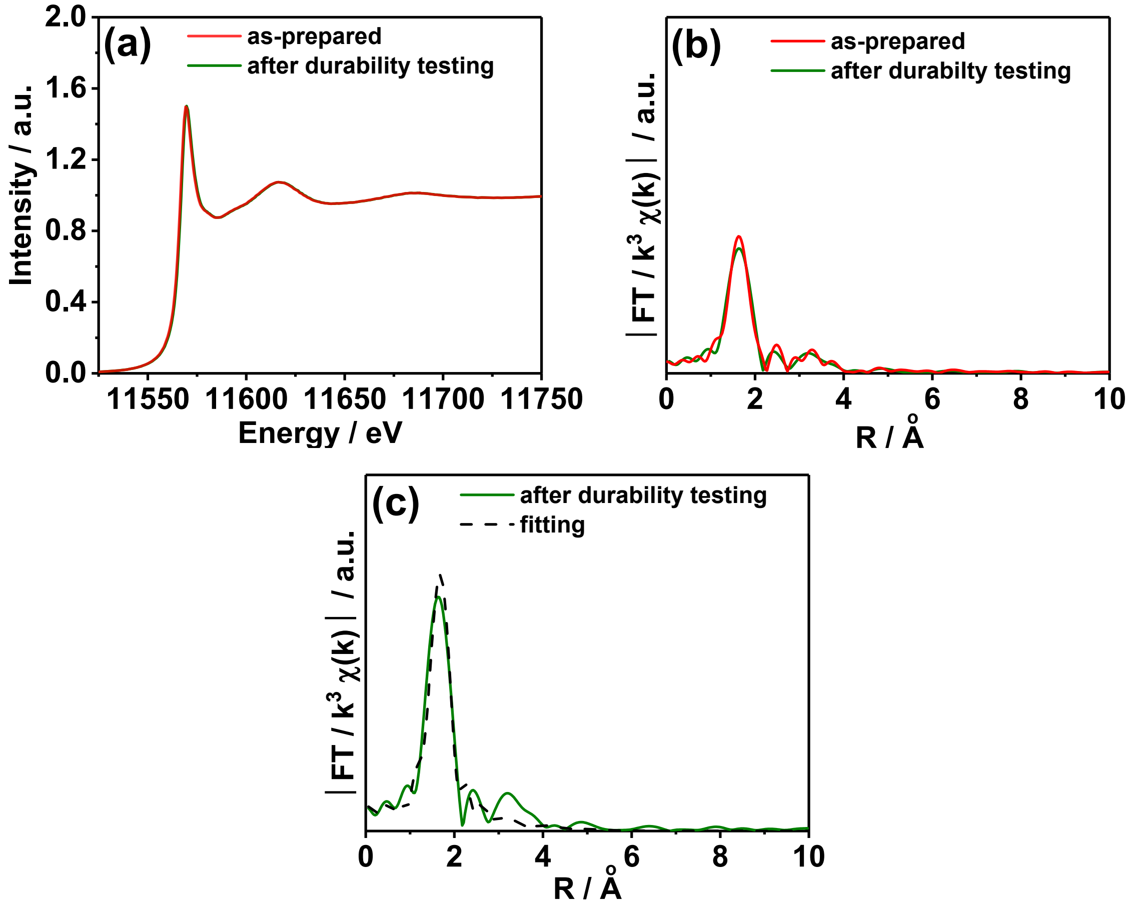

Fig. S15 (a) XANES and (b) FT-EXAFS of the Pt L_3-edge of Pt SASs/AG before and after durability testing (without phase correction); (c) Corresponding EXAFS fitting curve of Pt SASs/AG after durability testing.

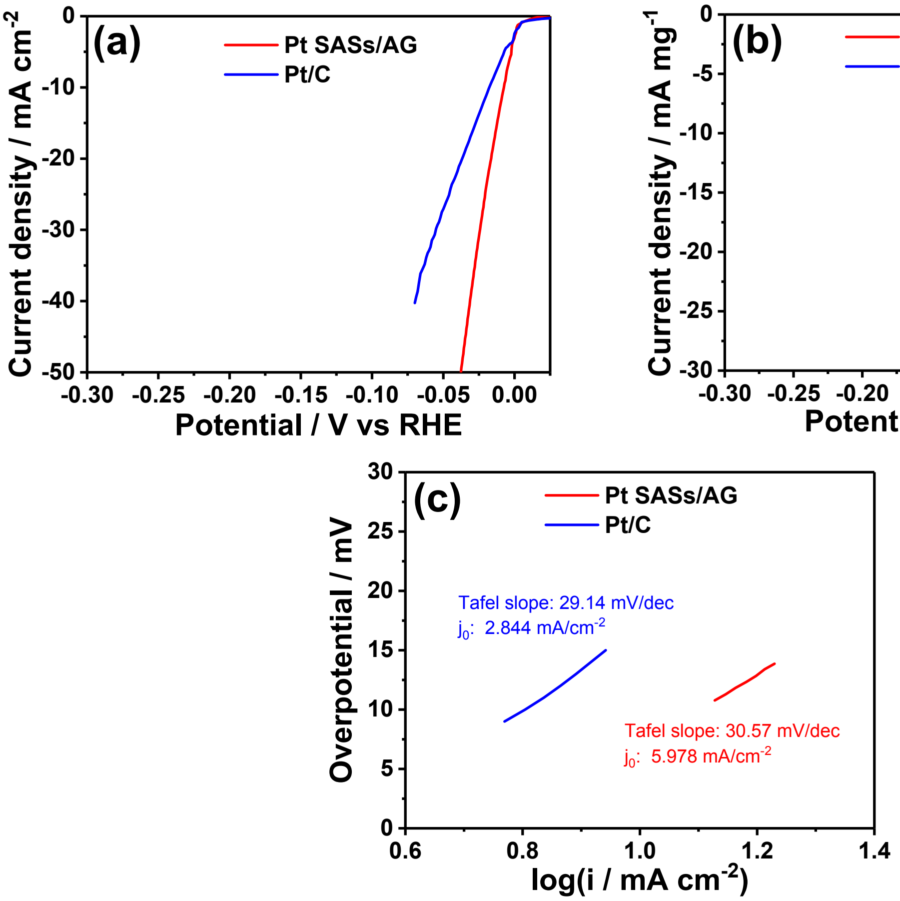

Fig. S16 LSV curves of Pt SASs/AG and Pt/C with current density normalized to the (a) geometry area and (b) mass of Pt in 1 M KOH at 2 mV s^{-1} respectively; (c) Tafel plots of Pt SASs/AG and Pt/C in 1 M KOH

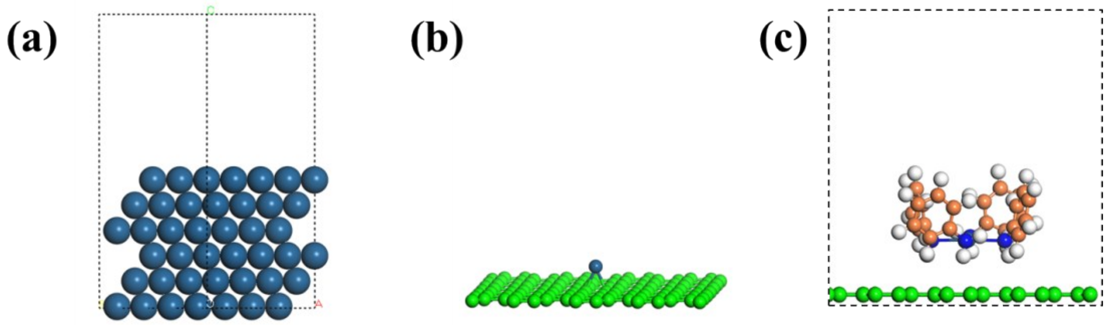

Fig. S17 DFT calculation models (side views) of (a) Pt (111), (b) Pt_{ab}/G and (c) Pt SASs/AG.

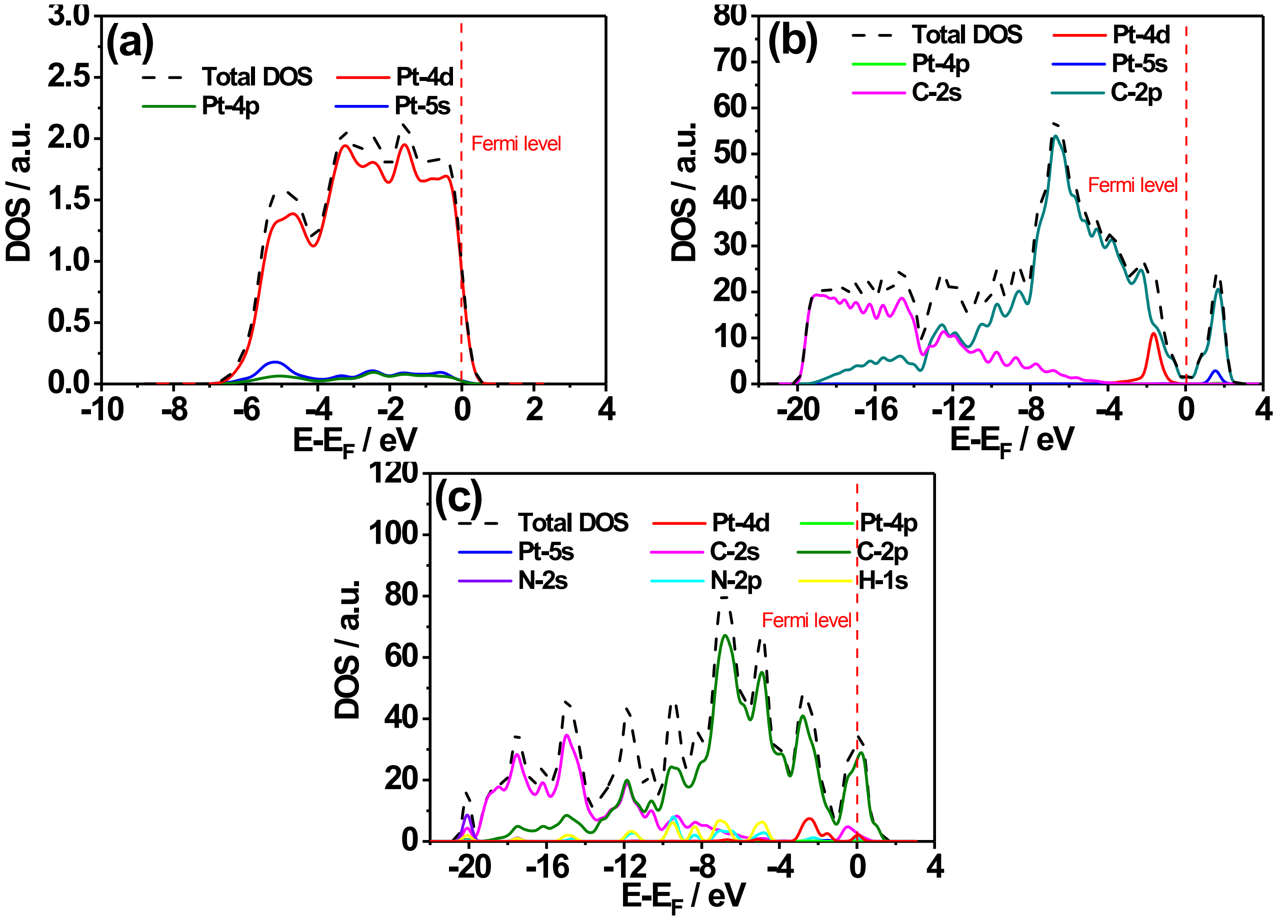

Fig. S18 Total DOS of (a) Pt (111), (b) Pt_{ab}/G and (c) Pt SASs/AG.

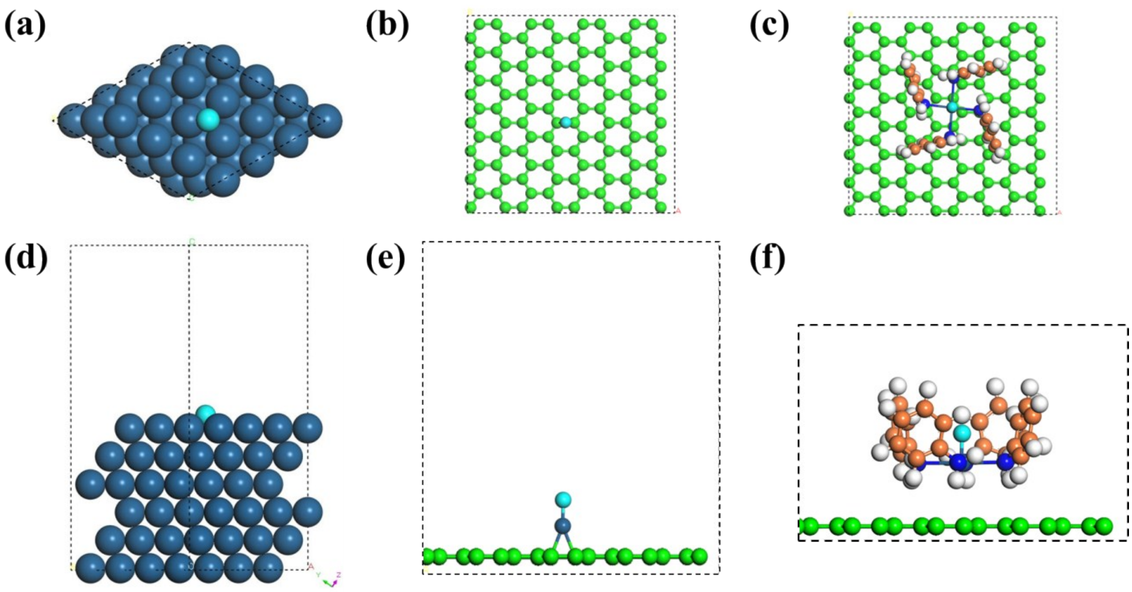

Fig. S19 (a, d) Pt (111), (b. e) Pt_{ab}/G and (c,f) Pt SASs/AG with the H absorption modelfor the DFT calculations.